Computer Simulation of Offset Printing: III. Effect of Ink Feed Mechanism

Shem M. Chou* and Ted Niemiro*

Keywords: Lithography, Inker, Simulation, Dynamics, Print Quality

Abstract: This is the third of a series of papers in computer simulation of web offset printing process. This paper focuses on the effect of ink feed mechanism on press performance. The following five ink feed mechanisms were simulated: ductor-feed open fountain, continuous-feed open fountain, digital injector, anilox keyless inker, and positive-feed keyless inker.

A bar graph test form was used to study the dynamic behavior of various inkers. It was found that both press time constant and incubation period are independent of any change of ink feedrate, if the ink film thickness is used as the control variable. Dynamic properties vary with the magnitude and direction of ink feedrate change, if the optical density is used as the control variable. Differences between the two controlling methods result from the non-linear relationship between optical density and ink film thickness. It was also found that ink feed mechanism influences significantly the dynamic behavior of a press. The press time constant was found to increase with decreasing image coverage for all of the inkers except the positive-feed keyless inker, of which it is independent of image coverage. The press equipped with a continuous-feed open fountain overall responds fastest to a step change of ink feedrate, while the press with a digital injector exhibits the slowest response. Keyless inkers tend to respond faster than conventional, keyed inkers for very light formes.

A T-bar/triangle/stripe test form was specifically designed for appraising print quality attributes such as ghosting, starvation, and ink film thickness uniformity. A ditch and ridge pattern is typical of the T-bar image produced by conventional, keyed inkers, but the ridge vanishes when printed by keyless inkers. Ink feed mechanism was found to have a negligible effect on the magnitude of ghost, and the positive feed keyless inker

* Goss Graphic Systems, 700 Oakmont Lane, Westmont, IL 60559-5546
Tel: (630) 850-6461, Fax: (630) 850-6415, E-mail: smchou@gossgraphic.com

exhibited a lower starvation than the other inkers. The results from the stripe test target demonstrate that ghosting is indeed augmented if a ghost image from one form roller overlaps with that from another. The ink film thickness is the least uniform with the ductor-feed open fountain inker, apparently due to its intermittent feed of ink to the roller train. The ink film thickness of an image produced by the anilox keyless inker is much more strongly dependent upon the image coverage of the plate than the other inkers, because of a poor inker design. The simulation results and the effect of ink feed mechanism on press performance will be presented. Selection of a proper inker for a specific print job will also be discussed.

Introduction

This is the third of a series of papers in computer simulation of web offset printing process. The oscillation of vibrators was ignored in the first paper (Chou and Bain, 1996). The effect of vibrator oscillation on the ink distribution behavior of an inker was studied in the second paper (Chou, 1997). Press dynamics and print quality were used in those papers as the criteria for appraising the capability of an inker design. The former characterizes the rate of a press responding to a change of ink feedrate. The faster the press can respond, the faster the process can reach the steady state. That is, the more stable is the process and hence the less print waste it will produce. The latter characterizes the image-related variations of ink film thickness in the printing and across-the-press directions. An ideal inker should be able to deliver a uniform ink film to the plate regardless of the image layout of the plate.

It was found in the previous papers that the printed ink film thickness, rates of ink flowing through each of the three ink form rollers and to the web, and quantity of ink built up in the inker all followed a first order differential equation for step changes of ink feedrate, from which the press time constant and incubation period were derived. If the ink film thickness is used as the control variable, both press time constant and incubation period were found to be independent of the ink feedrate change, regardless of its direction and magnitude. If the optical density is used as the control variable, the press responds to a step increase in ink feedrate faster than a step decrease and, in some cases, the response to a large change may be faster than a small one. These differences in the response of an inker to the ink feedrate change were attributed to the non-linear relationship between optical density and ink film thickness (Chou and Harbin, 1991). The oscillation of vibrators was found to have a negligible effect on this behavior.

It was also found that the press time constant and mean ink residence time are both inversely proportional to the image coverage in the absence of vibrator oscillation. When the vibrators oscillate, the relationship between press time constant and the reciprocal of image coverage becomes increasingly less linear with increasing magnitude of vibrator oscillation, while the linear relationship between mean ink residence time and image coverage is not affected at all. This behavior was attributed

to the lateral flow of ink across the inking zones of the roller train by the oscillation of vibrators. In general, the ink throughput rate is increased in low image coverage zones but decreased in high coverage zones by the lateral flow of ink. The press time constant is accordingly reduced in low image coverage zones but increases in high coverage zones. In any case, the general trend of increasing press time constant with decreasing image coverage still holds. Because the mean ink residence time is defined as the ratio of ink volume in the inker to ink throughput rate (MacPhee et al., 1986), its relationship with image coverage is not affected.

There are two image-related variations of ink film thickness that cannot be compensated by ink key adjustment, namely, ghosting and starvation. Ghosting is an ink film thickness variation in the printing direction due to different sizes of plate cylinder and ink form rollers in conjunction with an improper layout of images. Starvation is an ink film thickness variation in the across-the-press direction due to the finite width of ink keys in conjunction with a large step change in the image coverage within an ink key. The oscillation of vibrators significantly reduces starvation, but has a negligible effect on ghosting. The larger the stroke length and/or the faster the oscillation rate, the less the starvation.

The aforementioned findings were obtained on the assumption that the amount of ink fed to the pickup roller is directly proportional to the image coverage of each inking zone. The complex behavior of ink transfer from the ink fountain to the roller train was ignored. In general, most inkers are equipped with a slow-speed fountain roller and the remaining rollers and cylinders are running at the press speed. The amount of ink transferred from the fountain roller to the pickup roller will vary with time until the steady state is reached. The complex behavior of ink film split between fountain and pickup rollers will definitely affect press dynamics and probably quality of printed images. This paper will present the methodology that simulates various ink feed mechanisms and focus on its effect on press performance.

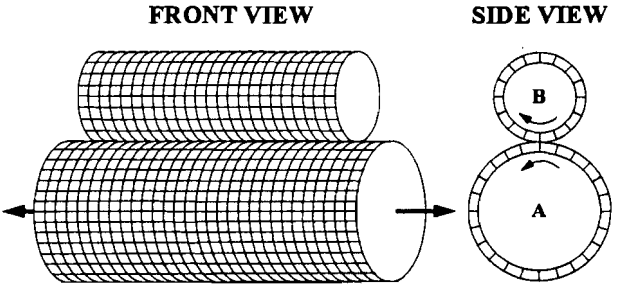

Figure 1. Schematic diagram showing the roller surfaces divided into many small cells. Each cell contains ink film thickness information. Roller A is a vibrator.

Computer Simulation Methodology

The methodology of simulating ink distribution between inking rollers and cylinders has been discussed in detail in previous papers (Chou and Bain, 1996; Chou, 1997). It is briefly reviewed here to maintain the integrity of this paper. In the computer simulation, the surfaces of all inking rollers and plate and blanket cylinders are divided into 0.25" by 0.25" cells, as shown schematically in Figure 1. The ink film thicknesses at the exit of any inking roller nip, e.g. ink distribution from Vibrator A to Roller B as illustrated in Figure 1, can be expressed by the following equations:

$$H'_B(i,j) = S_{AB}\left[H_A(k,l) + H_B(i,j)\right] \quad (1)$$

and

$$H'_A(k,l) = (1 - S_{AB})\left[H_A(k,l) + H_B(i,j)\right] \quad (2)$$

with,

H_A : thickness of inflow ink film on Roller A,
H_B : thickness of inflow ink film on Roller B,
H'_A : thickness of outflow ink film on Roller A,
H'_B : thickness of outflow ink film on Roller B,
i, k : indices specifying the cell positions around the rollers,
j, l : indices specifying the cell positions across the rollers,
S_{AB} : split ratio specifying the fraction of ink in the roller nip distributed to Roller B.

The relationship between indices j and l is governed by the oscillation of vibrators and can be expressed by the following equation.

$$l = j + L_S \sin(2\pi\nu N + \phi) / N_C \quad (3)$$

with,

L_S : stroke length,
ν : oscillation rate,
ϕ : phase angle,
N : number of plate cylinder revolutions, i.e., time of printing,
N_C : number of cells per unit length across the rollers.

The oscillation rate of 1:6, that is, one cycle of oscillation every 6 plate cylinder revolutions, and the stroke lengths of 5/4" were used in this work. The phase angles of 0, 120, and 240 degrees were adopted for the three vibrators to minimize the net momentum of axial movement.

For nips involving an ink form roller and the plate cylinder, the fractional image coverage of each cell on the plate cylinder has to be included in the distribution equations as follows, on the assumption that there is no mechanical dot gain.

$$H'_P(i,j) = S_{FP}\left[H_P(i,j) + H_F(k,j)\right] \quad (4)$$

and

$$H'_F(k,j) = F(i,j)(1-S_{FP})\left[H_P(i,j) + H_F(k,j)\right] + \left[1 - F(i,j)\right]H_F(k,j) \quad (5)$$

with,

H_P : thickness of inflow ink film on the plate cylinder,
H_F : thickness of inflow ink film on the ink form roller,
H'_P : thickness of outflow ink film on the plate cylinder,
H'_F : thickness of outflow ink film on the ink form roller,
$F(i, j)$: fractional image coverage of cell $P(i, j)$ on the plate cylinder.
S_{FP} : split ratio specifying the fraction of ink in the nip transferred to the plate.

The first term on the right of Eq. (5) is the quantity of ink left after distribution on the ink form roller corresponding to the image area. The second term is the quantity of ink on the ink form roller corresponding to the non-image area that is not involved in ink distribution.

Figures 2 to 6 illustrate respectively the schematic diagrams of the presses equipped with different ink feed mechanisms: ductor-feed open fountain, continuous-feed open fountain, digital injector, anilox keyless inker, and positive-feed keyless inker. The main structure of those presses, based on the World 16 press manufactured by Goss Graphic Systems, remains the same for the purpose of comparing the ink feed mechanism only. Some inkers have a couple of additional rollers as required by the rotation of inking rollers.

Ductor-Feed Open Fountain

Because paste inks are very difficult to shear at high speeds, traditional inking system designs incorporate some type of slow-speed metering device (MacPhee, 1998). Most often this comprises a V-shaped open fountain and a slow-moving fountain roller. Metering is accomplished by the fountain roller that carries a presumably precise amount of ink through the gap formed between fountain blade and fountain roller. A portion of the metered ink film is then transferred from the fountain roller (FR) to the faster-moving pickup roller (PR) via a friction-driven ductor roller (DR) that swings back and forth between fountain roller and pickup roller, as shown schematically in Figure 2.

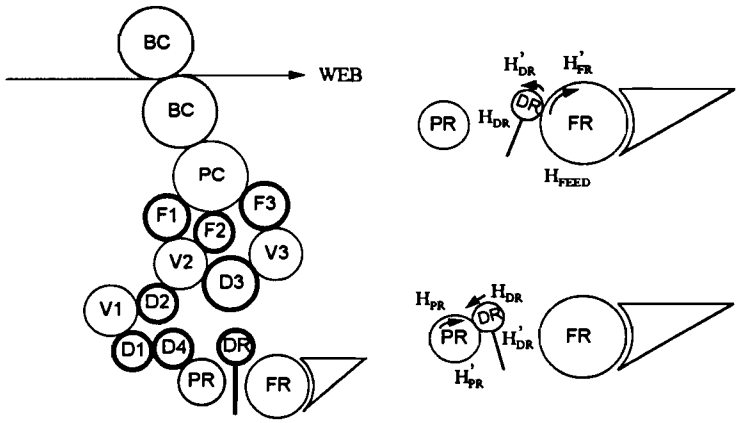

Figure 2. Schematic diagram illustrating the roller configuration and ink feed mechanism of the simulated press with a ductor-feed open fountain.

The ductor is in contact with the fountain roller during the first half of ductor cycle. A small strip of ink is transferred from the fountain roller to the ductor. Because the thickness of ink film on the fountain roller entering the nip is governed by the gap between fountain blade and fountain roller, regardless of the remaining ink on the return-side of fountain roller, ink distribution between the two rollers can be expressed by the following equations:

$$H'_{DR}(i,j) = S_{FD}\left[H_{Feed}(j) + H_{DR}(i,j)\right] \tag{6}$$

and

$$H'_{FR}(k,j) = (1 - S_{FD})\left[H_{Feed}(j) + H_{DR}(i,j)\right] \tag{7}$$

with,

H_{DR} : thickness of inflow ink film on the ductor,
H_{Feed} : thickness of metered ink film on the fountain roller,
H'_{DR} : thickness of outflow ink film on the ductor,
H'_{FR} : thickness of outflow ink film on the fountain roller,
S_{FD} : split ratio specifying the fraction of ink in the roller nip distributed to the ductor.

Because the thickness of metered ink film is determined by the gap between fountain blade and fountain roller, it is a constant before entering the nip. It may vary across the press as the gap is adjusted according to the image coverage of each inking zone. So, only the index j that specifies the cell position across the roller is needed to designate the thickness of metered ink film on the fountain roller, H_{Feed}.

During the second half of ductor cycle the ductor is swung into contact with the pickup roller and some of the ink on it is transferred to the roller train. The distribution of ink between ductor and pickup roller can be expressed by:

$$H'_{PR}(i,j) = S_{DP}\left[H_{PR}(i,j) + H_{DR}(k,j)\right] \tag{8}$$

and

$$H'_{DR}(k,j) = (1 - S_{DP})\left[H_{PR}(i,j) + H_{DR}(k,j)\right] \tag{9}$$

with,

H_{PR} : thickness of inflow ink film on the pickup roller,
H'_{PR} : thickness of outflow ink film on the pickup roller,
S_{DP} : split ratio specifying the fraction of ink in the roller nip distributed to the pickup roller.

It was assumed in this work that the ductor cycle is equal to 10 plate cylinder revolutions and the surface speed ratio of pickup roller to fountain roller is equal to 40. The fountain roller moves through a sweep angle of 34° to transfer a strip of ink to the ductor during the first 5 plate cylinder revolutions. At the start of the next 5 plate cylinder revolutions, the ductor swings into contact with the pickup roller for 7 ductor roller revolutions. It was further assumed that the ductor roller was accelerated instantly to the speed of fountain roller or pickup roller and there was no skidding between them. The split ratios, S_{FD} and S_{DP}, are both assumed to be 0.5.

The thickness of metered ink film on the fountain roller is not only a function of the gap between fountain blade and fountain roller, but also depends on the fountain roller speed, ink viscosity and temperature, and ink level in the fountain (VanKanegan, 1998). The deflection of rotating fountain roller and/or fountain blade may vary the gap clearance between fountain blade and fountain roller. Dampening water feedback may also interfere with ink transfer to the pickup roller or the metering capability of the ink fountain. Because of these variables, the thickness of metered ink film on the fountain roller is not precisely controlled by the gap between fountain blade and fountain roller. In the case of surface speed ratio of pickup roller to fountain roller equal to 40, any error in the thickness of metered ink film will translate into a 2.5% of that error in the printed ink film thickness. In other words, the setting of ink keys is more tolerant with the slow-moving fountain roller. This is probably another reason why the fountain roller rotates at a slower speed. A calibration curve is definitely required to define the relationship between metered ink film thickness and gap clearance. Each ink may demand its own calibration curve. These variables affecting the thickness of metered ink film were intentionally ignored in this work to simplify the simulation.

Continuous-Feed Open Fountain

The intermittent transfer of ink from the fountain roller to the roller train via the ductor generates large disturbances in the ink film thickness throughout the train. A longer roller train is demanded to attenuate these disturbances. To overcome these disadvantages and to simplify the inking system, the ductor-feed open fountain was often replaced with the continuous-feed open fountain, as illustrated in Figure 3.

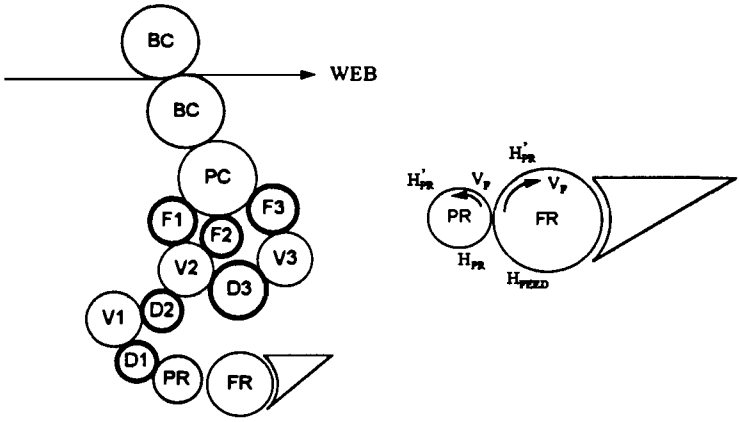

Figure 3. Schematic diagram illustrating the roller configuration and ink feed mechanism of the simulated press with a continuous-feed open fountain.

Because the pickup and fountain rollers are running at different speeds, a gap must be set between them to prevent wear and tear of rollers. This gap is approximately 0.005" in most presses. The transfer of ink from the fountain roller to the pickup roller can be expressed by:

$$V_P H'_{PR}(i,j) = S_{FP}\left[V_F H_{Feed}(j) + V_P H_{PR}(i,j)\right] \tag{10}$$

which can be rearranged into

$$H'_{PR}(i,j) = S_{FP}\left[(V_F / V_P) H_{Feed}(j) + H_{PR}(i,j)\right] \tag{11}$$

with,

V_P : the surface speed of pickup roller which is equal to the press speed,
V_F : the surface speed of fountain roller,

The term on the left of Eq. (10) is the quantity of ink on the pickup roller per unit time after exiting the nip. The terms in the bracket on the right of Eq. (10) are respectively

the quantities of ink on the fountain and pickup rollers per unit time before entering the nip. Similarly, the amount of ink retaining on the fountain roller after split is expressed by the following equation:

$$H'_{FR}(k,j) = (1 - S_{FP}) \left[H_{Feed}(j) + (V_P / V_F) H_{PR}(i,j) \right] \quad (12)$$

Because there is a gap between fountain and pickup rollers, the pickup roller normally has a textured surface to plow out the ink from the fountain roller and to prevent roller slip. The split ratio, S_{FP}, is therefore strongly dependent upon the texture of pickup roller surface and the gap clearance. It was simply assumed to be equal to 0.5 in this work. The gap clearance between pickup and fountain rollers also affects the amount of ink transferred to the roller train. A 0.001" change in the gap may result in a change of 0.2 in the optical density (VanKanegan, 1998). The surface speed ratio of pickup roller to fountain roller was assumed to be equal to 40.

As discussed in the previous section, the same factors will also influence the thickness of metered ink film on the fountain roller. In addition, the zero point of ink feedrate is uncertain because of the gap between fountain and pickup rollers, and hence the setting of zero point is poorly reproducible. This will affect particularly the optical density of printed image in low coverage zones and also the pre-setting of ink keys. These difficulties were also neglected for the time being in this work.

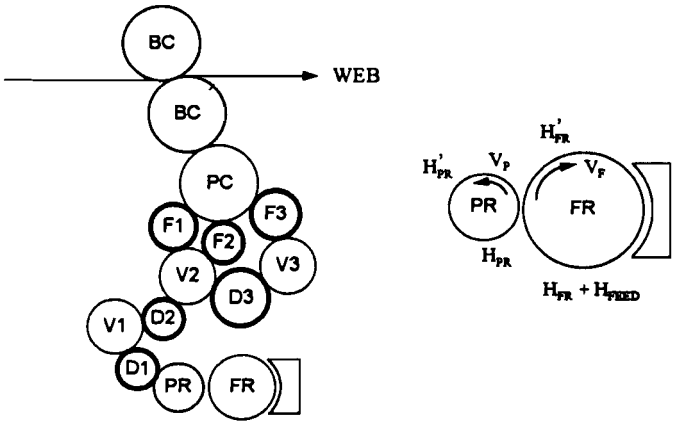

Figure 4. Schematic diagram illustrating the roller configuration and ink feed mechanism of the simulated press with a digital injector.

Digital Injector

Modern newspaper printing presses commonly incorporate piston or digital injectors. The amount of ink delivered to the inking system by a piston injector is controlled by

the length of the piston plunger stroke. Digital injectors utilize, for example, gear pumps in conjunction with valves to regulate an extremely precise amount of ink to the fountain roller through an ink rail. It is generally not easy to set the zero point of and to adjust the piston injector for very small image coverage (VanKanegan, 1998). In comparison, the zero point of a digital injector can be precisely set by turning off the valve. Piston injectors are therefore gradually replaced with digital injectors.

Figure 4 illustrates schematically the press equipped with a digital injector. If the fountain roller runs at very high speeds, ink tends to deposit and accumulate on the smoothing blade of ink rail due to the viscoelastic properties of paste inks (Chou, 1992). The accumulated ink will be sooner or later carried out by the fountain roller, causing a surge of ink supply to the plate. So, the fountain roller normally runs at slower speeds and a gap must be set between fountain and pickup rollers, similar to the continuous-feed open fountain. Because the metered ink film is always added to the residual ink on the fountain roller, the distribution of ink can be expressed as follows:

$$H'_{PR}(i,j) = S_{FP}\left[(V_F/V_P)\left(H_{Feed}(j) + H_{FR}(k,j)\right) + H_{PR}(i,j)\right] \qquad (13)$$

and

$$H'_{FR}(k,j) = (1 - S_{FP})\left[\left(H_{Feed}(j) + H_{FR}(k,j)\right) + (V_P/V_F)\,H_{PR}(i,j)\right] \qquad (14)$$

with,

H_{FR} : thickness of residual ink film on the fountain roller,
H_{Feed} : thickness of metered ink film added to the fountain roller,

Eq. (14) and (15) are similar to Eq. (12) and (13), except the term representing the thickness of metered ink film on the fountain roller. The split ratio, S_{FP}, is also strongly dependent upon the texture of pickup roller surface and the gap clearance. It was again assumed to be equal to 0.5. The surface speed ratio of pickup roller to fountain roller was assumed to be equal to 20 in this study.

Because the rate of ink feed is controlled by gear pumps and valves and inks are incompressible fluids, the quantity of ink metered to the fountain roller is independent of ink viscosity and temperature. Moreover, the calibration curve defining the relationship between key setting and ink feedrate is not required. These advantages account for the popularity of digital injectors in the newspaper industry. However, it is not easy to clean the digital injector for color change and the dried debris of commercial inks may plug the gear pump. These fears have taken the shine out of the digital injector for application to the commercial presses.

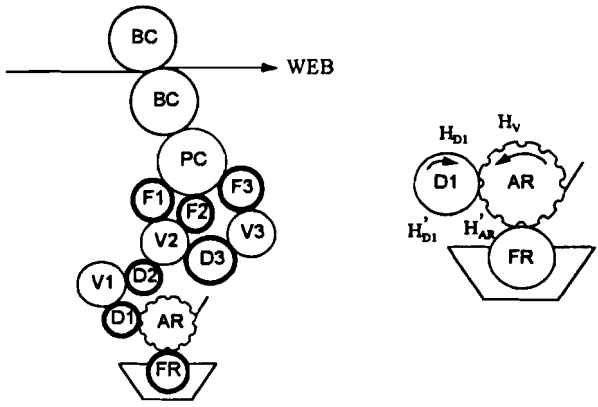

Figure 5. Schematic diagram illustrating the roller configuration and ink feed mechanism of the simulated press with an anilox keyless inker.

Anilox Keyless Inker

There are more than one thousand ink keys in a modern double-width newspaper press line. Ink key adjustments are often a nightmare and paper waste is always high. Press manufacturers began, more than thirty years ago, developing keyless processes to simplify press operation and to reduce paper waste. The concept of anilox keyless inker, shown schematically in Figure 5, was borrowed from flexography and had been adopted in many newspaper pressrooms (Fadner and Bain, 1987; Fadner and Bain, 1989).

In this anilox keyless process, the fountain roller forces the ink into the cells of anilox roller and excess ink is scraped off from the anilox roller surface by a doctor blade. The quantity of ink transferred to the distribution roller, D_1, is supposed to be proportional to the cell volume of the anilox roller and a fraction of ink is transferred back to the land area of the anilox roller from the distribution roller (Fadner, 1990). The anilox roller is moving at the press speed. So, the distribution of ink between anilox and distribution rollers can be expressed by:

$$H'_{D1}(i,j) = A_L (1 - S_{DA}) H_{D1}(i,j) + (1 - A_L) H_{D1}(i,j) + F_{AN} H_V \qquad (15)$$

and

$$H'_{AR}(k,j) = A_L S_{DA} H_{D1}(i,j) + (1 - F_{AN}) H_V \qquad (16)$$

with,

H_V : cell volume per unit area of anilox roller in units of ink film thickness,

F_{AN} : fraction of ink transferred out of the cells of anilox roller to the distribution roller,

A_L : fraction of land area of anilox roller,

S_{DA} : split ratio specifying the fraction of ink on the distribution roller transferred back to the land of anilox roller.

The cell volume per unit area of anilox roller is independent of the position in both printing and across-the-roller directions and hence H_V is used in Eq. (15) and (16) without indices. The first term on the right side of Eq. (15) is the ink left after split on the distribution roller corresponding to the land area of anilox roller. The second term is the inflow ink on the distribution roller corresponding to the cells of anilox roller, which remains intact during ink film splitting. The third term is the quantity of ink flowing out of the cells of anilox roller and transferring to the distribution roller.

The quantity of ink flowing out of the cells of anilox roller is supposedly controlled by the cell volume, as in flexography with fluid inks. It is rather determined in lithography by the viscosity of inks which is much higher than that of flexographic inks. It was reported that lithographic inks with a lower viscosity and a negligible yield value indeed performed much better on the anilox keyless offset presses (Chou and Bain, 1988). Ink transfer out of the cells of anilox roller is further complicated by the emulsified fountain solution, which changes the viscosity of ink and in many cases interferes with ink transfer if it can not survive the extremely high shear imposed by the doctor blade (Chou and Bain, 1995). Temperature is another factor affecting the metering capability of anilox roller. The roller flat setting between anilox and distribution rollers affects the shear conditions in the roller nip and hence the amount of ink transferred out of the cells. In general, the larger the roller flat, the more ink is transferred out of the cells. Wear of anilox roller also changes the cell volume and the fraction of ink flowing out of the cells. These factors were not considered in this work to simplify the computer simulation. It was assumed that a constant fraction of ink is transferred out of the cells, regardless of ink rheology and the presence of emulsified water. This constant, F_{AN}, was assumed to be equal to 0.8. The fraction of land area, A_L, was assumed to be equal to 0.36 and the split ratio, S_{DA}, was 0.5.

Positive-Feed Keyless Inker

One of the major drawbacks of anilox keyless process is its lack of shade control. If the print density is outside the range of target density, pressmen could not do anything to correct that. In other words, the printers have to rely on the ink makers to supply specially formulated, batch-to-batch consistent inks. To overcome this drawback, Goss Graphic Systems has developed a different process called positive-feed keyless process. This system utilizes a digital injector to feed an ink uniformly across the press and the excess ink is scraped off the inker by a doctor blade, as shown schematically in Figure 6. The scraped ink is circulated back to the reservoir and subsequently re-introduced to the digital injector. Print density can be easily varied by adjusting the

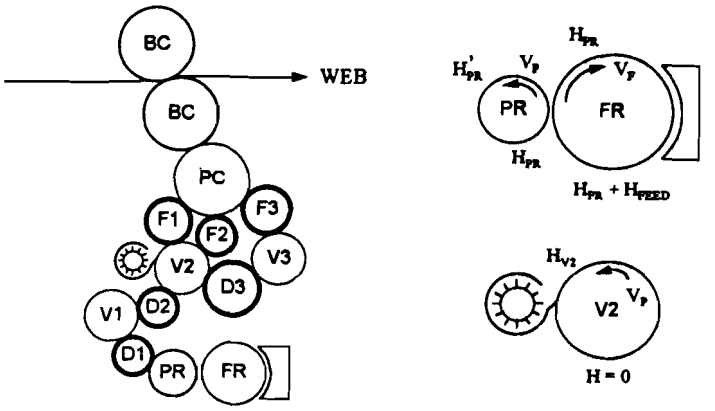

Figure 6. Schematic diagram illustrating the roller configuration and ink feed mechanism of the simulated press with a positive-feed keyless inker.

feedrate of digital injector. Equations governing the ink feed to the roller train are as follows:

$$H'_{PR}(i,j) = S_{FP}\left[(V_F/V_P)\left(H_{Feed} + H_{FR}(k,j)\right) + H_{PR}(i,j)\right] \qquad (17)$$

and

$$H'_{FR}(k,j) = (1 - S_{FP})\left[\left(H_{Feed} + H_{FR}(k,j)\right) + (V_P/V_F)\,H_{PR}(i,j)\right] \qquad (18)$$

Eq. (17) and (18) are similar to Eq. (13) and (14), except that the index is taken away from the ink feed term, H_{Feed}, because the ink feed is uniform across the press. The split ratio, S_{FP}, was assumed to be equal to 0.5. The surface speed ratio of pickup roller to fountain roller was assumed to be equal to 20. It was also assumed that the excess ink was completely removed from the roller train by the doctor blade.

Our experience in the field has proven that the positive-feed keyless press could print many standard injector inks without any difficulty. Specially formulated inks are not required. Target density can always be achieved by adjusting the ink feedrate. Press operation becomes very simple and the paper waste is minimal. Free water might occasionally appear in the ink fountain and interfered with ink transfer. However, this problem can be solved easily with the advent of single fluid lithography.

Press Dynamics

The bar graph shown in Figure 7 was used as the test form to study the dynamic behavior of an inker. The left and right pages of the bar graph test form consist of solid

and halftone bars, respectively. The image coverages of those bars, as indicated by the number underneath each bar, vary from 10% to 100% in an increment of 10%. The width of each bar is equal to the width of an ink fountain key, and there are six cells across each bar. The ink feedrate to each inking zone was set in proportion to the image coverage of that zone for the conventional, keyed inkers. In comparison, an ink feedrate just enough to cover 100% image was set uniformly across the press for the keyless inkers. The effect of vibrator oscillation on the ink throughput rate was not taken into consideration in this work. The simulation process, starting with a clean inker, included four stages of varying ink feedrate. The target thickness of ink film on the substrate was 1 μm at the first stage, increased to 1.5 μm at the second stage, brought back to 1 μm at the third stage, and the ink feed was completely terminated at the fourth stage. The press was allowed to run for 520 plate cylinder revolutions at each stage, except for the digital injector and positive-feed keyless inkers which require longer response time. The latter two presses were allowed to run for 1120 plate cylinder revolutions at each stage. It is in fact impossible to vary the ink feedrate of an anilox keyless press during printing. This constraint was ignored in this work.

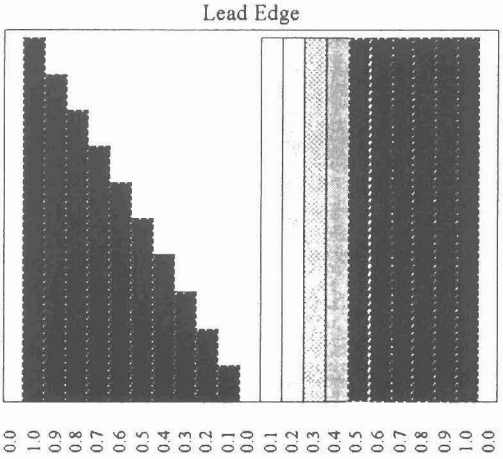

Figure 7. Bar graph used as the test form to study the dynamic behavior of an inker. The number underneath each bar indicates the image coverage of that ink input zone.

Ink Film Thickness Profile

Figure 8 shows the ink film thickness profiles of the solid bar with 100% image coverage obtained from the last 20 plate cylinder revolutions in the first stage. The corresponding standard deviations of ink film thickness are summarized in Table I as a function of image coverage. These results indicate that the uniformity of ink film thickness is strongly dependent upon the ink feed mechanism. The order of inkers

producing ink film with decreasing uniformity is as follows: continuous-feed open fountain > positive-feed keyless inker ≈ digital injector >> ductor-feed open fountain >> anilox keyless inker.

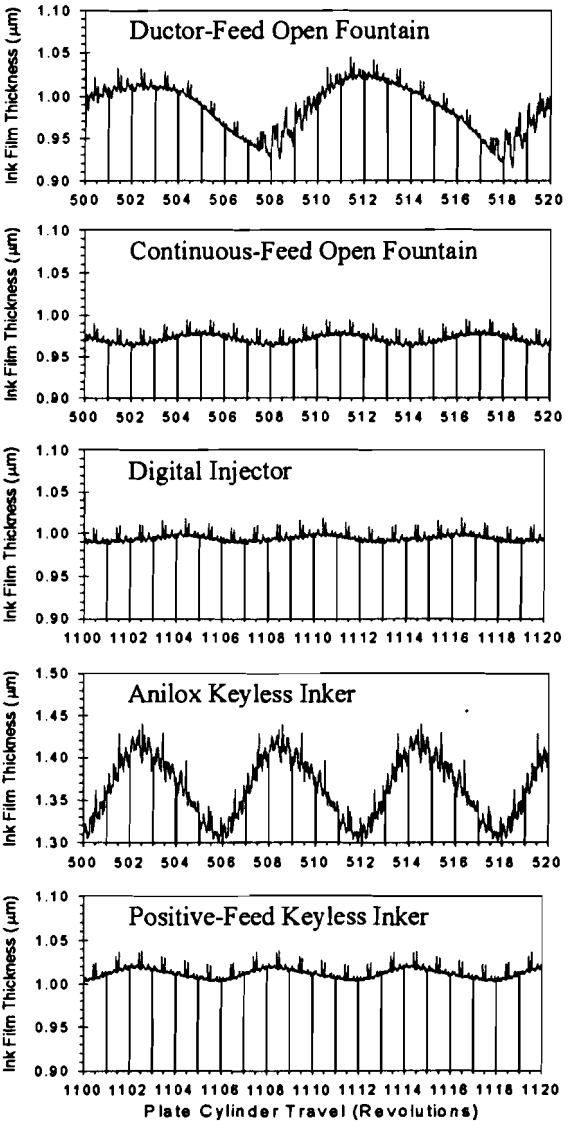

Figure 8. Ink film thickness profile of the 100% solid bar obtained from last 20 plate cylinder revolutions of the presses with various ink feed mechanisms.

Table 1. Effect of ink feed mechanism on the standard deviations of ink film thickness as a function of image coverage.

Image Coverage	Ductor Open Ftn.	Continuous Open Ftn.	Digital Injector	Anilox Keyless	Positive-Feed Keyless
0.1	0.0050	0.0032	0.0055	0.0846	0.0037
0.2	0.0093	0.0058	0.0093	0.0984	0.0062
0.3	0.0122	0.0054	0.0090	0.0848	0.0049
0.4	0.0149	0.0039	0.0073	0.0668	0.0046
0.5	0.0189	0.0066	0.0083	0.0521	0.0074
0.6	0.0235	0.0104	0.0111	0.0422	0.0116
0.7	0.0280	0.0127	0.0130	0.0343	0.0143
0.8	0.0299	0.0112	0.0113	0.0231	0.0127
0.9	0.0313	0.0078	0.0078	0.0177	0.0086
1.0	0.0304	0.0075	0.0126	0.1424	0.0124

The ink film thickness fluctuates around the target value of 1 μm for all of the inkers except the anilox keyless inker which varies from 1.30 to 1.43 μm. In theory, a given thickness of ink film can be achieved by an inker with a zonal control of ink feedrate, that is, ink film thickness is independent of image coverage. In the keyless offset process ink is fed to the inking system uniformly across the press, regardless of image coverage, at a rate that is just enough to cover 100% image. The excess ink in the inking zones with an image coverage less than 100% must be removed from the inker to prevent the ink from accumulating in the roller train. The nature of lithographic press design requires a number of rollers existing between plate cylinder and scraping or anilox roller. These rollers act as a reservoir for storing some of the excess ink. In other words, the excess ink can not be completely removed from the inker. The lower the image coverage, the larger quantity of ink is stored there. A portion of that ink is subsequently transferred to the plate, resulting in the increased thickness of printed ink film with decreasing image coverage. This variation of ink film thickness with image coverage also depends on the location of anilox roller in the anilox keyless inker or the scraping roller in the positive-feed keyless inker. The farther the anilox or scraping roller away from the plate cylinder, the larger the reservoir and hence the greater the variation of ink film thickness with image coverage (Niemiro and Chou, 1998). The anilox roller in this study is 5 rollers away from the plate cylinder, while the scraping roller of positive-feed keyless inker is only 1 roller away. It is predicted that a much thicker ink film will be produced by the anilox keyless offset. The oscillation of vibrators will also transport the excess ink from low to high image coverage zones, resulting in an ink film thicker than the target value at high image coverage zones. These phenomena are clearly illustrated in Figure 9.

Close examination of Figure 8 shows that the period of sinusoidal ink film thickness

profile is 6 plate cylinder revolutions for all of the inkers except the ductor-feed open fountain whose period is 10 plate cylinder revolutions. The former behavior is attributed to the oscillation rate of vibrators (Chou, 1997) and the latter to the ductor cycle. The ductor cycle of the ductor-feed open fountain apparently overpowers the oscillation of vibrators. The ink film produced by the intermittent ink feed of the ductor-feed open fountain is therefore the least uniform. These results may account for the trend in the industry that the ductor-feed open fountain is gradually replaced by the continuous-feed open fountain.

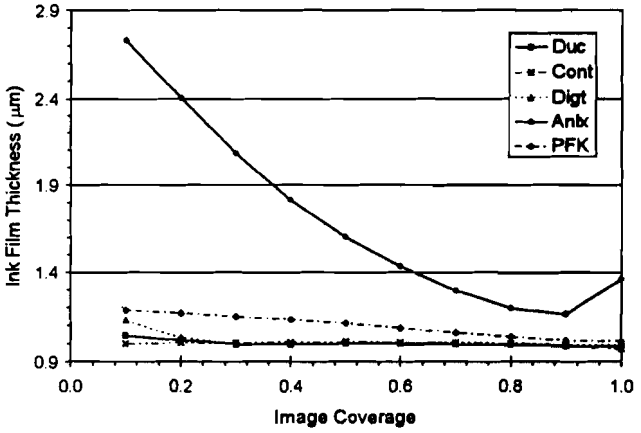

Figure 9. Effect of ink feed mechanism on the ink film thickness as a function of image coverage obtained from solid bars of the bar graph.

Dynamic Behavior

Figure 10 illustrates the average printed ink film thicknesses of the 50% solid bar as a function of plate cylinder revolutions obtained from simulating the inkers with the ductor-feed open fountain and the digital injector. The solid lines are drawn through the data points according to the first order differential equation reported by Neuman and Almendinger (1978) as follows.

$$H = H_o + (H_\infty - H_o)\left[1 - \exp[-(N - N_d)/\tau_p]\right] \qquad (19)$$

with,

H : thickness of ink film on the substrate,
H_o : initial ink film thickness before a step change of ink feedrate,

H_∞ : steady-state ink film thickness after a step change of ink feedrate,
N : number of plate cylinder revolutions or time of printing,
N_d : incubation period or delay time which is the time elapsed before the output begins to respond to the step change.
τ_p : press time constant characterizing how fast the process reaches the steady state, e.g. the inker will achieve 63.2%, 95.0%, and 99.3% of the steady state after 1, 3, and 5 τ_p impressions, respectively.

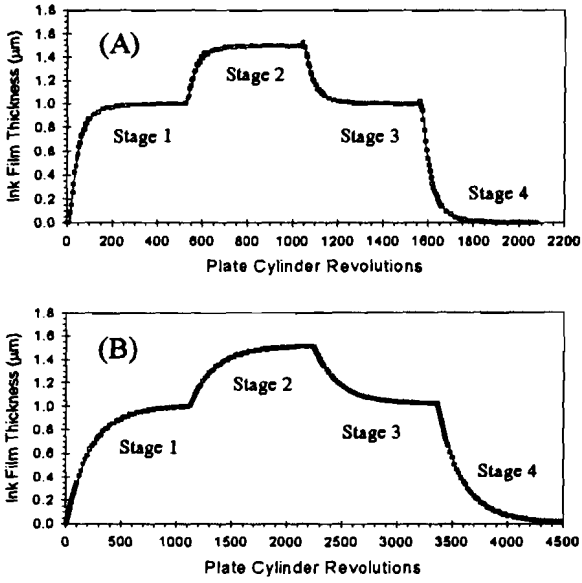

Figure 10. Dynamic behavior of printed ink film of the 50% solid bar obtained from the presses equipped with (A) a ductor-feed open fountain and (B) a digital injector.

Eq. (19) obviously fits the ink film thickness data very well for the press equipped with either a ductor-feed open fountain or a digital injector. Excellent agreement between ink film thickness data and Eq. (19) was also found for the other inkers. The press time constants and incubation periods derived from Eq. (19) for the solid bars produced by the press with the ductor-feed open fountain are listed in Tables 2 and 3, respectively. Statistical data are also included in the tables. It is noted that both press time constants and incubation periods of all four stages are, from the statistical viewpoint, the same for each image coverage. Similar results were also obtained from the halftone bars as well as those of the other inkers. The incubation periods and press time constants obtained from the rates of ink flowing through each of the three form

rollers and to the web, and the quantity of ink built up in the inker are also independent of ink feedrate change for all of the inkers studied in this report. All of these results indicate that the dynamic response of an inker is independent of the ink feedrate change, regardless of its direction and magnitude. The ink feed mechanism does not affect this behavior.

Table 2. Press time constant of solid bars as a function of image coverage obtained from the analysis of ink film thickness for the four inking stages of the press with a ductor-feed open fountain.

Image Coverage	Stage of Ink Feed 1	2	3	4	Mean	Standard Deviation
0.1	112.42	112.72	112.94	112.51	112.65	0.200
0.2	92.35	92.64	92.45	92.44	92.47	0.107
0.3	70.26	70.59	70.30	70.36	70.38	0.127
0.4	54.33	54.69	54.44	54.43	54.47	0.131
0.5	44.47	44.77	44.60	44.55	44.59	0.110
0.6	38.36	38.63	38.51	38.45	38.49	0.100
0.7	34.49	34.74	34.64	34.58	34.61	0.094
0.8	32.50	32.74	32.64	32.61	32.62	0.086
0.9	34.10	34.22	34.23	34.16	34.18	0.054
1.0	47.52	46.90	47.33	47.41	47.29	0.234

Table 3. Incubation period of solid bars as a function of image coverage obtained from the analysis of ink film thickness for the four inking stages of the press with a ductor-feed open fountain.

Image Coverage	Stage of Ink Feed 1	2	3	4	Mean	Standard Deviation
0.1	19.46	19.76	19.58	20.24	19.76	0.298
0.2	12.67	12.99	13.12	13.41	13.05	0.267
0.3	10.81	11.23	11.38	11.57	11.25	0.280
0.4	11.02	11.45	11.57	11.79	11.46	0.282
0.5	11.33	11.83	11.90	12.13	11.80	0.290
0.6	11.39	11.92	11.97	11.19	11.87	0.293
0.7	11.26	11.81	11.87	12.06	11.75	0.295
0.8	10.85	11.41	11.46	11.64	11.34	0.292
0.9	9.82	10.54	10.40	10.68	10.36	0.325
1.0	8.26	10.41	10.02	9.36	9.51	0.816

Table 4. Press time constant of presses with various ink feed mechanisms as a function of image coverage.

Image Coverage	Ductor Open Ftn.	Continuous Open Ftn.	Digital Injector	Anilox Keyless	Positive-Feed Keyless
0.1	112.65	19.47	588.84	25.25	93.97
0.2	92.47	17.75	431.72	23.46	93.96
0.3	70.38	16.09	320.69	21.10	93.94
0.4	54.47	14.74	257.14	18.81	93.94
0.5	44.59	13.66	219.93	16.89	93.93
0.6	38.49	12.79	196.50	15.39	93.92
0.7	34.61	12.08	181.09	14.30	93.92
0.8	32.62	11.52	172.43	13.75	93.92
0.9	34.18	11.39	175.92	14.66	93.92
1.0	47.29	13.48	218.55	19.30	94.03
R^2	0.8196	0.7835	0.9042	0.6987	

Table 5. Incubation period of presses with various ink feed mechanisms as a function of image coverage.

Image Coverage	Ductor Open Ftn.	Continuous Open Ftn.	Digital Injector	Anilox Keyless	Positive-Feed Keyless
0.1	19.76	6.24	25.71	4.72	1.37
0.2	13.05	6.05	9.46	4.46	1.29
0.3	11.25	6.01	5.51	4.34	1.24
0.4	11.46	5.99	5.53	4.32	1.20
0.5	11.80	5.99	5.90	4.35	1.17
0.6	11.87	5.98	5.94	4.37	1.17
0.7	11.75	5.98	5.58	4.37	1.17
0.8	11.34	5.96	4.62	4.31	1.17
0.9	10.36	5.84	2.39	4.09	1.18
1.0	9.51	5.50	0.39	3.67	1.28

Tables 4 and 5 summarize the averaged press time constant and incubation period obtained from the solid bars of presses with various ink feed mechanisms. Both press time constant and incubation period generally increase with decreasing image coverage for all of the inkers except the positive-feed keyless inker, which are practically independent of the image coverage. These results indicate that the press dynamics is strongly dependent upon the ink feed mechanism. The order of inkers responding to an ink feedrate change is as follows: continuous-feed open fountain >

anilox keyless inker > ductor-feed open fountain > positive-feed keyless inker >> digital injector.

The ink feedrate to the fountain roller or by the anilox roller to achieve a printed ink film of 1 μm thick at the 100% image coverage is 172.6 μm, 348.7 μm, 20 μm, 75.5 μm, or 2.5 μm for the presses with a ductor-feed open fountain, a continuous-feed open fountain, a digital injector, a positive-feed keyless inker, or an anilox keyless inker, respectively. These ink feedrates are much higher than 1 μm used in the previous papers (Chou and Bain 1996; Chou, 1997). Except the anilox keyless inker, the other inkers all have a slow-speed fountain roller and their press time constant is directly related to the ink feedrate. The higher the ink feedrate, the faster the press reaches the steady state. Because the residual ink after splitting does not accumulate on the fountain roller in the continuous-feed and ductor-feed open fountain inkers, their ink feedrates can be set much higher than those of digital injector and positive-feed keyless inker. The positive-feed keyless inker has a faster response time than the digital injector, because of its higher ink feedrate of which a significant portion of ink is scraped off the inker.

It was found in the previous papers (Chou and Bain, 1996; Chou, 1997) that the press time constant is proportional to the reciprocal of image coverage in the absence of vibrator oscillation; and this linear relationship becomes worse, the more vigorous the oscillation of vibrators. This departure from the linear relationship was ascribed to the lateral flow of ink from high to low coverage zones, caused by the oscillation of vibrators. Similar behavior, as indicated by the linear regression coefficients R^2 in Table 4, was observed in this study for all of the inkers except the positive-feed keyless ink.

It was also found in the previous papers (Chou and Bain, 1996; Chou, 1997) that if the optical density is used as the control variable, the response of press to a step increase in ink feedrate is faster than a step decrease; the response to a large increase in ink feedrate is faster than a small increase; and the response to a small decrease in ink feedrate is faster than a large decrease. These phenomena were ascribed to the non-linear relationship between optical density and ink film thickness (Chou and Harbin, 1991). To study the effect of ink feed mechanism on press dynamics using a densitometer as a means of process control, the ink film thickness data were converted into optical density according to the equation proposed by Calabro and Savagnone (1983) as follows.

$$\frac{1}{D} = \frac{1}{D_S} + \left(\frac{m}{H}\right)^n \qquad (20)$$

with,

D : optical density,

H : ink film thickness,

D_s : saturation density which is the density of an ink film of infinite thickness or the maximum density that can be achieved by an ink,

m : density smoothness parameter which characterizes how fast the ink mileage curve approaches the saturation density,

n : power law index which is generally implemented to improve the fitness of equation to the experimental data.

Table 6. Press time constant of solid bars as a function of image coverage obtained from the analysis of optical density for the four inking stages of the presses with a ductor-feed open fountain and a positive-feed keyless inker.

Image	Ductor-feed Open Fountain				Positive-feed Keyless Inker			
Coverage	0-1μ	1-0μ	1-1.5μ	1.5-1μ	0-1μ	1-0μ	1-1.5μ	1.5-1μ
0.1	105.82	125.89	111.24	114.60	89.03	105.73	92.76	95.27
0.2	86.48	103.87	91.32	93.88	89.03	105.71	92.76	95.25
0.3	65.85	79.31	69.58	71.39	89.03	105.69	92.75	95.23
0.4	51.24	61.25	53.95	55.22	89.03	105.67	92.74	95.22
0.5	12.21	49.87	44.23	45.19	89.03	105.65	92.74	95.21
0.6	36.60	42.87	38.20	38.99	89.04	105.63	92.74	95.19
0.7	32.99	38.49	34.37	35.05	89.04	105.61	92.75	95.18
0.8	31.07	36.39	32.38	33.03	89.05	105.59	92.75	95.18
0.9	32.35	38.60	33.79	34.70	89.06	105.58	92.76	95.18
1.0	44.57	54.03	46.20	48.07	89.15	105.70	92.86	95.27

The ink mileage parameters selected to convert a 1.0-μm ink film on a standard newsprint, whose optical density of 0.21, to an optical density of 1.0 are as follows: $D_s = 1.59$, $m = 0.5972$, $n = 0.8965$. An equation identical to Eq. (19) was used to fit the optical density data versus plate cylinder revolutions, from which the incubation period and press time constant were derived. Table 6 lists, as an example, the press time constant obtained from the solid bars of the presses with a ductor-feed open fountain and a positive-feed keyless inker. The results show that the press time constant is also independent of image coverage for the positive-feed keyless inker, but varies with image coverage for the ductor-feed open fountain inker. Close examination of Table 6 data indicates that the response to a step increase in ink feedrate is faster than a step decrease; the response to a large increase in ink feedrate is faster than a small increase; and the response to a small decrease in ink feedrate is faster than a large decrease. Similar behavior was also observed for the other inkers. It is concluded that if the optical density is used as the control variable, the dynamic response of press is controlled by the magnitude and direction of ink feedrate change. This conclusion

is consistent with that obtained previously (Chou and Bain, 1996; Chou, 1997) and can be applied to the press with any ink feed mechanism.

Mean Ink Residence Time

MacPhee et al. (1986) defined the mean ink residence time as the ratio of the ink volume in the inker to the ink throughput rate. It is a measure of the time that the ink spends on the rollers. It was found that the mean ink residence time is inversely proportional to the image coverage and the oscillation of vibrators does not affect this relationship at all (Chou, 1997). That is, the ink spends much more time on the inking rollers for light coverage formes and hence may emulsify too much water on the sheetfed press or tack up on the web press, making it very difficult to print those formes (MacPhee et al., 1986).

Table 7. Mean ink residence time of presses with various ink feed mechanisms as a function of image coverage.

Image Coverage	Ductor Open Ftn.	Continuous Open Ftn.	Digital Injector	Anilox Keyless Shutdown	Printing	Positive-Feed Keyless
0.1	203.69	169.73	169.93	151.79	16.64	8.66
0.2	110.14	88.94	88.90	78.70	14.67	8.72
0.3	79.26	62.17	62.16	54.61	13.11	8.78
0.4	63.77	48.76	48.76	42.57	11.89	8.85
0.5	54.53	40.76	40.76	35.39	10.95	8.90
0.6	48.49	35.53	35.53	30.70	10.21	8.95
0.7	44.20	31.81	31.81	27.36	9.62	9.00
0.8	40.98	29.01	29.02	24.82	9.15	9.05
0.9	38.52	26.87	26.85	22.77	8.87	9.09
1.0	35.88	24.90	24.66	20.79	9.08	8.99
R^2	1.0000	1.0000	1.0000	1.0000	0.8759	0.8974

Because the ink residence time is critical to the operation of lithographic printing process, it is important to determine if the ink feed mechanism affects the mean ink residence time. Table 7 summarizes the mean ink residence time as a function of image coverage for the presses with various ink feed mechanisms. The results indicate that the mean ink residence time is inversely proportional to the image coverage for all of the inkers except the positive-feed keyless inker, of which it increases linearly with image coverage. The linear regression coefficients, R^2, of mean ink residence time versus image coverage are also listed. A perfect linear relationship was observed for all of the conventional inkers, whereas the linear relationship is somewhat less perfect for the keyless inkers.

When ink feed mechanism is taken into consideration in the simulation program, mean ink residence time becomes dramatically different from press time constant, as shown by the data in Table 4 and 7. The former is related to the ink throughput rate, whereas the latter is related to the ink feedrate.

The mean ink residence times are slightly longer for the press with a ductor-feed open fountain than that with a continuous-feed open fountain or a digital injector. The latter two presses have the same mean ink residence times. This behavior can be attributed to the size of inker. The former inker has a slightly larger size than the latter two identical inkers. Keyless presses differ from conventional presses in that a uniform ink film is fed to the plate and excess ink is scraped off the inker. There are two outlets of the ink flow path during keyless printing, ink printed on the substrate and ink scraped off the inker. The effective ink throughput rate is therefore much higher for keyless presses and hence the mean ink residence times are much shorter. At press shutdown, the anilox roller is thrown off the inking system and there remains only one outlet, ink printed on the substrate. This situation is similar to the conventional presses. It is therefore predicted that the mean ink residence times for the anilox keyless inker at press shutdown should be similar to those of conventional presses. This is proven by the data in Table 7. The mean ink residence times are slightly shorter for the anilox keyless inker because it has one roller less than the presses with a digital injector and a continuous-feed open fountain. As for the positive-keyless inker, the doctor blade is always engaged whether during printing or at press shutdown. So, the mean ink residence time is the same for both situations.

Because in the keyless process the scraped ink is returned to the ink fountain, mixed up with fresh ink there, and then re-introduced to the inking system, the effect of solvent loss to the atmosphere on ink tacking-up is minimized. The scraped ink also carries the emulsified water back to the ink fountain, mixed up with fresh ink there, and then re-introduced to the inking system. The dampening water gradually accumulates in the ink fountain until the steady state is reached or the ink fails to emulsify any more water. It may become more difficult to control ink-water balance in the former case due to the excess, emulsified water carried by the ink. The ink feed becomes unpredictable in the latter case due to free water interference. Extremely high shear imposed by the doctor blade of anilox keyless press may easily squeeze water out of the emulsion ink, which will interfere with subsequent ink transfer and make the printing process unpredictable. In summary, the keyless inkers may have less ink tacking-up but more emulsification problems than the conventional inkers.

Ink Flow Ratio

It has been shown in the previous papers (Chou, 1997) that the 100-0-0 inker produces less severe ghosting than the 60-20-20 inker and the oscillation of vibrators has a negligible effect on the magnitude of ghost. These phenomena were related to the ink flow ratio. The more ink is contributed to the plate by the first ink form roller,

the less severe is the ghosting. The magnitude of vibrator oscillation was found to have a negligible effect on the ink flow ratio and hence a negligible effect on the magnitude of ghost.

Figure 11 illustrates the ink flow ratio of various presses as a function of image coverage. The ink flow ratio data essentially overlap one another at each image coverage for all of the inkers, though those obtained from the anilox keyless inker differ slightly. Those data are also in excellent agreement with the theoretical values predicted by the method proposed by Guerrette (1985), as shown by the lines drawn through the data in the chart. These results indicate that the ink feed mechanism does not have any significant effect on the ink flow ratio. It is therefore predicted that the ink feed mechanism should not affect the magnitude of ghost either. Figure 11 also shows that all of the presses studied in this work have a 40-40-20 inker, compared with the 100-0-0 and 60-20-20 inkers of the original World 16 press. It is also predicted that the presses in this study will produce a more severe ghosting than World 16 press. The data in Table 8 of this paper and in Tables 6 and 7 of the previous paper (Chou, 1997) indeed prove these predictions.

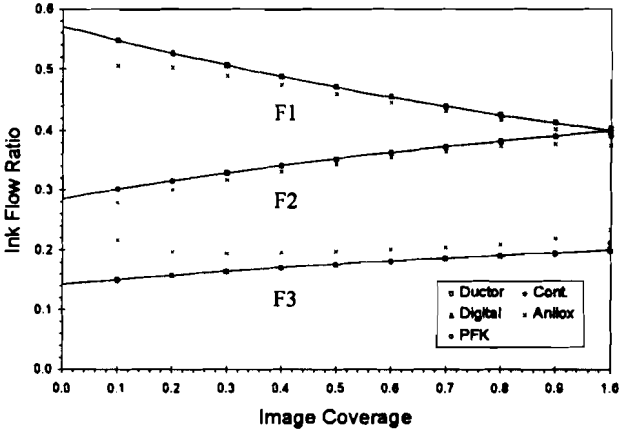

Figure 11. Effect of ink feed mechanism on ink flow ratio as a function of image coverage obtained from solid bars of the bar graph.

Print Quality

The T-bar/triangle/stripe test form illustrated schematically in Figure 12 was designed for evaluating the capability of a press to produce high quality prints. The T-bar test target is used to determine the magnitude of ghost produced by each of the three ink

form rollers and the magnitude of starvation. Ghosting and starvation are defined as a measure of non-uniformity of ink film thickness in the printing and across-the-press directions, respectively (Chou, 1997). The triangle test target is used to determine an inker's capability of delivering an image-coverage-independent ink film to the plate. The stripe test target, similar to that reported by Scheuter and Rech (1970), is used to demonstrate that ghosting can be augmented by overlapping ghost images resulting from multiple ink form rollers due to poor selection of roller size.

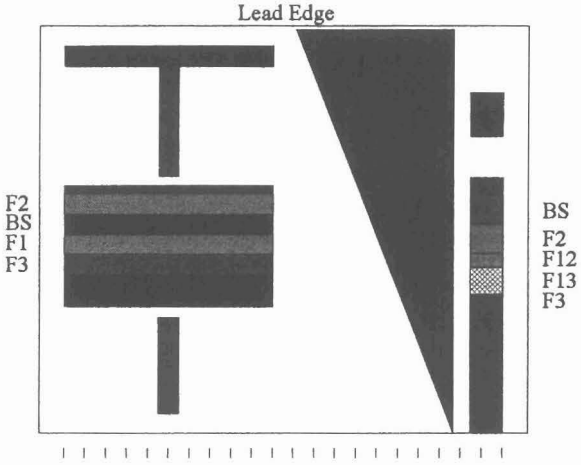

Figure 12. T-bar/triangle/stripe test form used to appraise print quality attributes produced by an inker.

T-Bar Test Target

It has been shown that a ditch and ridge pattern of the printed T-bar image is common to the inkers equipped with a keyed ink input device (Chou, 1997) and the ridge vanishes with keyless inkers (Chou, et al., 1996). Consistent results were obtained in this study as illustrated in Figure 13. The ditch and ridge pattern is shown clearly in Figure 13A for the press equipped with a continuous-feed open fountain. Similar pattern was also obtained from presses with a ductor-feed open fountain and a digital injector. The ridge no longer exists in the prints produced by both keyless presses (Figure 13B and 13C). The formation of ditch and ridge pattern is due to the finite width of ink keys in the conventional, keyed inkers. If there is an abrupt change in the image coverage in an inking zone, the high coverage area is underfed but the low coverage area is overfed, because the ink feedrate is generally set according to the image coverage of that inking zone. This unbalanced ink feed can be lessened by the oscillation of vibrators (Chou, 1997), but cannot be eliminated completely. The overfed ink corresponding to the low coverage area in that particular inking zone is

removed from the inking system in the keyless inkers, resulting in the disappearance of ridges.

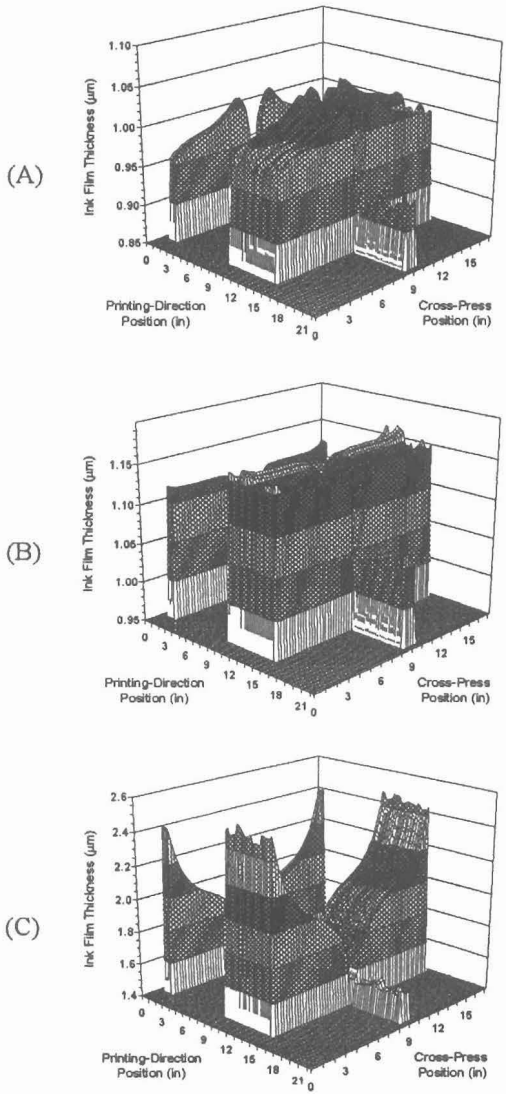

Figure 13. 3-D column charts of the T-bar image obtained from the presses equipped with (A) a continuous-feed open fountain, (B) a positive-feed keyless inker, and (C) an anilox keyless inker.

The horizontal bars produced by the positive-feed keyless inker are relatively flat (Figure 13B), while those produced by the anilox keyless inker are characterized by steep hills on both edges (Figure 13C). Those peculiar steep hills result from the relatively large reservoir between anilox roller and plate cylinder that can store a huge amount of excess ink. In addition, there is a 0%-coverage zone on each side of the T-bar (Figure 12), which has the same ink feedrate as that of 100%-coverage zones and will contribute additional ink to the edges of the T-bar via the oscillation of vibrators. It is predicted that those steep hills will gradually flatten out as the number of rollers between plate cylinder and anilox roller reduces and will be investigated in the future.

Analysis of the T-bar test target has been discussed in detail in the previous paper (Chou, 1997). The magnitude of ghost can be calculated by the following equation,

$$G = \left[1 - \frac{H_{Fi}}{H_{BS}} \right] * 100 \qquad (21)$$

with,

G : percentage ghost,
H_{Fi} : ink film thickness of ghost image produced by the form roller Fi,
H_{BS} : ink film thickness of the baseline image.

The percentage starvation can be calculated by the following equation,

$$S = \left[1 - \frac{H_D}{H_R} \right] * 100 \qquad (22)$$

with,

S : percentage starvation,
H_D : ink film thickness of the ditch,
H_R : ink film thickness of the ridge.

Because ridges do not exist in the T-bar image produced by either keyless inker, the ink film thickness of the plateau instead of ridge is used in the calculation of starvation. Table 8 lists the percentage ghost and starvation of the T-bar image produced by various inkers. The results indicate that the ink feed mechanism has a negligible effect on the magnitude of ghost. This conclusion is consistent with the prediction made on the basis of ink flow ratio analysis discussed previously. However, the ink feed mechanism has a significant impact on the magnitude of starvation. The ranking of inkers with respect to starvation is as follows: positive-feed keyless inker > continuous-feed open fountain > ductor-feed open fountain > digital injector > anilox

keyless inker. It is predicted that the performance of anilox keyless inker will be significantly improved by a reduction in the number of rollers between plate cylinder and anilox roller.

Table 8. Effect of ink feed mechanism on the percentage ghost and starvation of the T-bar image.

	Ductor Open Ftn.	Continuous Open Ftn.	Digital Injector	Anilox Keyless	Positive-Feed Keyless
%G(F1)	1.70	1.69	1.68	1.68	1.51
%G(F2)	1.70	1.70	1.69	1.67	1.78
%G(F3)	2.12	2.11	2.11	2.11	2.19
%S	10.77	9.63	11.01	17.45	7.43

Triangle Test Target

The triangle test target is a very powerful tool to determine an inker's capability of producing an image-coverage-independent image. Compared with the abrupt change in the image coverage of the T-bar test target, variation in the image coverage in each inking zones of the triangle test target is gradual, which can be evened up easily by the oscillation of vibrators. Figure 14 illustrates the effect of ink feed mechanism on the ink film thickness of triangle test target as a function of image coverage in each 1/4"

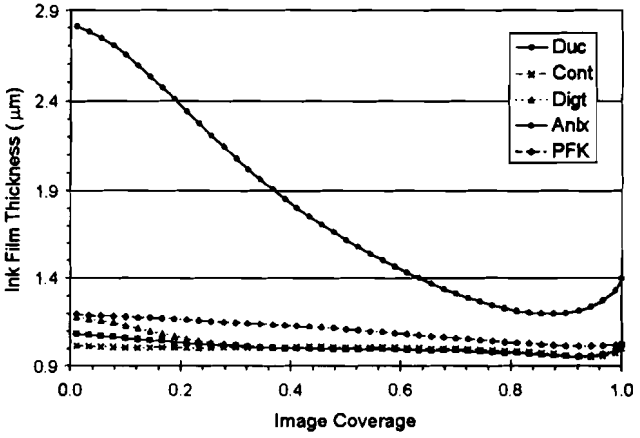

Figure 14. Effect of ink feed mechanism on the ink film thickness of triangle test target as a function of image coverage.

column. The thickness of ink film generally increases with decreasing image coverage in all of the cases studied in this work, indicating that the oscillation of vibrators with an oscillation rate of 1:6 and a stroke length of 5/4" can not completely smooth out the ink film delivered to the plate. This situation is even worse for the keyless inkers due to their uniform ink feed. The order of inkers producing an image-coverage-independent image is as follows: continuous-feed open fountain > ductor-feed open fountain > digital injector > positive-feed keyless inker >> anilox keyless inker. It is predicted that the performance of anilox keyless inker will be significantly improved by a reduction in the number of rollers between plate cylinder and anilox roller.

It is interesting to note by a close examination of Figures 9 and 14 that the ink film thickness curves essentially overlap one another. The former was obtained from the bar graph test form in which the image coverage is uniform within each inking zone. The latter was obtained from the triangle test target in which the image coverage varies within each inking zone. An implication from these results is that an extremely uniform ink film across the press can be achieved if the width of ink keys is infinitesimal. This, however, will be a nightmare for the engineers who design the press and for the pressmen who operate the press.

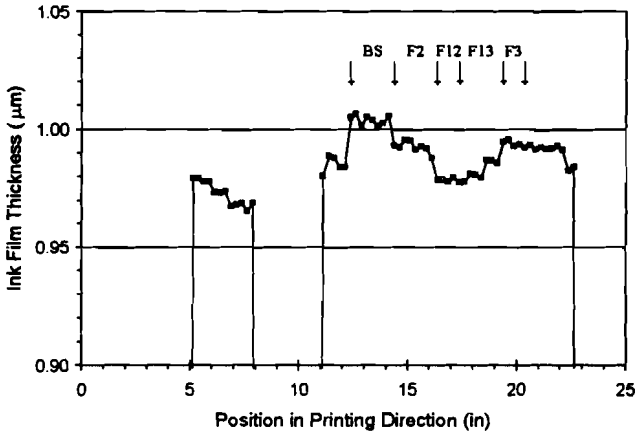

Figure 15. Ink film thickness profile of the stripe test target produced by the press equipped with a continuous-feed open fountain.

Stripe Test Target

The stripe test target is used to calculate the magnitude of compound ghost due to the overlap of ghost images from multiple ink form rollers. The test target is so designed

that the leading short block results in ghost images on the long block in such a way that the ghost image produced by F1 partially overlaps those produced by F2 and F3, respectively. Figure 15 shows, as an example, the ink film thickness profile of the stripe test target produced by the press equipped with a continuous-feed open fountain. The magnitude of ghost is calculated by an equation similar to Eq. (21). The results are summarized in Table 9.

The data in Table 9 lead to the conclusion that the ink feed mechanism has a negligible effect on the magnitude of ghost, whether it is a prime or compound ghost. This conclusion is consistent with that obtained from the analysis of T-bar test target. The results also show that the magnitude of compound ghost is about twice as much as that of prime ghost, indicating that the ink form rollers should differ in size as much as possible.

Table 9. Effect of ink feed mechanism on the percentage ghost and starvation of the stripe image.

	Ductor Open Ftn.	Continuous Open Ftn.	Digital Injector	Anilox Keyless	Positive-Feed Keyless
%G(F2)	0.97	1.14	1.12	1.07	1.12
%G(F12)	2.37	2.52	2.50	2.47	2.41
%G(F13)	2.29	2.18	2.19	2.22	2.28
%G(F3)	1.01	0.97	1.00	1.11	1.13

Ink Film Thickness Uniformity

Each test target discussed previously has its own focus. The bar graph is used to determine the response of a press to an ink feedrate change as well as the variation of printed ink film thickness with image coverage. The T-bar test target is used to determine the magnitude of ghost and starvation. The triangle test target is used to determine the variation of printed ink film thickness with image coverage or the capability of a press to print an image-coverage-independent image. The stripe test target is used to determine the magnitude of compound ghost. There is also a very important criterion for appraising print quality, that is, the uniformity of ink film of the entire page.

Table 10 lists the standard deviation of ink film thickness of various test target images from the last 20 print cylinder revolutions. The standard deviation is used as a measure of ink film thickness uniformity. It is not a surprise to observe that the anilox keyless inker makes the worst score in all categories due to its relatively huge inker size between plate cylinder and anilox roller. It is predicted that if the size of anilox keyless inker can be reduced by replacing the V2 drum with anilox roller and eliminating the

rollers D1, D2, and V1 (Figure 5), then print quality produced by this new inker will be as good as that by the positive-feed keyless inker (Niemiro and Chou, 1998). The positive-feed keyless inker has the best performance for an image that is relatively uniform across the press such as the stripe test target. The conventional, keyed inkers outperform keyless inkers in printing an image with a wide variation in the image coverage across the press such as the triangle test target and bar graph test form. For an image with a moderate variation in image coverage such as the T-bar test target, press performance of keyless inkers is as good as that of conventional, keyed inkers.

Table 10. Effect of ink feed mechanism on the standard deviation of ink film thickness of various test target images.

	Ductor Open Ftn.	Continuous Open Ftn.	Digital Injector	Anilox Keyless	Positive-Feed Keyless
T-bar	0.0418	0.0356	0.0390	0.2446	0.0369
Triangle	0.0315	0.0208	0.0173	0.3486	0.0501
Stripe	0.0324	0.0244	0.0296	0.1255	0.0137
Solid Bar	0.0272	0.0150	0.0179	0.3600	0.0523
Halftone Bar	0.0220	0.0089	0.0246	0.5122	0.0572

Implication in Inker Selection

Inkers can be classified into two categories according to the controllability of ink feed: passive and positive (VanKanegan, 1998). As discussed in the previous sections, the thickness of ink film metered by an open fountain is affected by the fountain roller speed, ink viscosity and temperature, and ink level. Dampening water feedback may interfere with ink transfer to the pickup roller. The fraction of ink transferred from the fountain roller to the pickup roller in the continuous-feed open fountain also varies with the gap between them and the surface texture of pickup roller. The residual ink on the fountain roller after split is carried back to the ink fountain, mixed with fresh ink therein, and carried out again by the fountain roller. The emulsified water transferred back to the ink fountain may alter its metering capability. This type of inker where the rate of ink fed to the roller train is, at the steady state, not equal to the rate of ink printed out to the paper is called passive-feed inker. Any variable affecting the thickness of metered ink film on the fountain roller will cause a significant change of the printed ink film thickness. It generally takes a relatively long time for all of those variables to reach their equilibrium values. Moreover, the zero point of ink feedrate is not well defined. A calibration curve is definitely needed to define the relationship between ink key setting and ink feedrate. These factors make the control of printing process very difficult and less predictable. It may translate into tremendous paper waste. Likewise, anilox keyless inker is a passive-feed inker.

In the piston or digital injector, ink is forced onto the fountain roller and the feedrate is controlled precisely by the injector, regardless of the amount of residual ink on the fountain roller. At the steady state, the rate of ink fed to the roller train is equal to the rate of ink printed out to the substrate and this type of inker is called positive-feed inker. Variables such as fountain roller speed, ink viscosity, and temperature do not affect this ink feed behavior. The zero point of ink feedrate can be set precisely and the calibration curve defining the relationship between ink key setting and ink feedrate is not required. This printing process with the positive-feed inker is therefore more stable and easier to control. Color reproduction is also more accurate. Likewise, positive-feed keyless inker is a positive-feed inker.

Because of the relatively low feedrate by the digital injector, it takes a much longer time for the ink to build up on the fountain roller to reach its equilibrium value, as indicated by the press time constants in Table 4. The slow press response may cause excess paper waste at the start-up. However, this can be overcome easily by pre-inking the roller train to shorten the makeready time. This has to be done carefully so that the roller train is not over inked. Once the makeready is done, any fine adjustment in ink key setting will not result in unacceptable prints because the key setting of a digital injector is very precise. Print quality produced by the digital injector is as good as that by the open fountain inkers. These results indicate that as long as the pre-inking is done correctly, digital injector will outperform open fountain inkers because the printing process with a digital injector is more stable and more predictable.

The response time of a positive-feed keyless press is faster than that of digital injector, but is still slower than that of open fountain and anilox keyless inkers. Nevertheless, the unique feature of positive-feed keyless inker allows pre-inking the roller train without the risk of over-inking, because the excess ink is continuously removed from the inking system by a scraper. This will shorten significantly the makeready time. Print quality produced by the positive-feed keyless inker is at least as good as that by the open fountain inkers, if the variation in image coverage is not too wide. Since the response time of the positive-feed keyless press is independent of image coverage and the ink feedrate can be varied to achieve the target density, the press operator can easily monitor the printing process with only one check point. In summary, the positive-feed keyless inker is superior to other inkers in most printing applications for its stable process and high quality printing.

Conclusions

The ink feed mechanism has a dramatic effect on the press dynamics and to a lesser extent on the magnitude of starvation. It has a negligible effect on the ink flow ratio and the magnitude of ghost. Press time constant increases with decreasing image coverage for all of the inkers except the positive-feed keyless inker, of which it is independent of image coverage. Starvation of a positive-feed keyless inker is less severe than that of the other inkers.

Very fast response to an ink feedrate change is a major advantage of the open fountain inkers. The ductor-feed open fountain has a slower response than the continuous-feed open fountain due to the intermittent ink feed of the former inker. Both open fountain systems are, however, a passive inker and many variables may influence the ink feedrate during printing, making it very difficult to maintain a stable printing process. Though digital injectors respond to an ink feedrate change much more slowly, this drawback can be overcome by pre-inking the roller train. The printing process with a digital injector is more stable and more predictable because digital injector is a positive inker and ink key setting is more precise. Color reproduction is also more accurate.

It is much easier to operate a keyless press than a conventional, keyed press. The response to an ink feedrate change of a keyless press is relatively fast. It is especially noted that press dynamics of a positive-feed keyless inker is independent of image coverage, making the process control much easier. Lack of shade control and more sensitivity to dampening water feedback interference are the major drawbacks of anilox keyless presses. Positive-feed keyless press is obviously a better choice than anilox keyless press.

The uniform ink feed of a keyless press results in the variation of printed ink film thickness with image coverage. This drawback is inherent in the lithographic press design. On the other hand, the removal of return ink by the scraper lessens the starvation problem, making the image layout more forgiving. Keyless press is more favorable to the conventional, keyed press if the image coverage is more or less uniform across the press or if the color reproduction is less critical such as newspaper printing.

Acknowledgment

The authors wish to acknowledge Mr. John MacPhee of Baldwin Technology and Mr. John Seymour of Quad Tech for providing insight information about the ink feed mechanism of ductor-feed open fountain. The authors are also very grateful to Mr. Eugene VanKanegan of Goss Graphic Systems for reviewing the manuscript and offering valuable suggestions.

Literature Cited

Calabro, G. and Savagnone, F.
1983 "A Method for Evaluating Printability," Adv. Printing Sci. Tech., Vol. 17, pp. 358-380.

Chou, S. M.
1992 "Viscosity Measurement of Viscoelastic Inks at High Shear Rates," TAGA Proceedings, pp. 388-408.

Chou, S. M.
1997 "Computer Simulation of Offset Printing: II. Effects of Vibrator Oscillation and Image Layout," TAGA Proceedings, pp. 94-118.

Chou, S. M. and Bain, L. J.
1988 "Rheological Characteristics: Keyless versus Conventional Litho Newsinks," TAGA Proceedings, pp. 354-386.

Chou, S. M. and Bain, L. J.
1995 "Theoretical and Practical Aspects of Single Fluid Lithography," TAGA Proceedings, pp. 121-139.

Chou, S. M. and Bain, L. J.
1996 "Computer Simulation of Offset Printing: I. Effects of Image Coverage and Ink Feedrate," TAGA Proceedings, pp. 523-547.

Chou, S. M., Bain, L. J., Durand, R., and Sanderson, E.
1996 "A Novel Printing Press for Waterless Lithography," Proceedings of 1996 International Printing and Graphic Arts Conference, pp. 165-174.

Chou, S. M. and Harbin, N.
1991 "Relationship Between Ink Mileage and Ink Transfer," TAGA Proceedings, pp. 405-432.

Fadner, T. A.
1990 "Prediction of Steady-State Operation in Keyless Lithography," TAGA Proceedings, pp. 363-392.

Fadner, T. A. and Bain, L. J
1987 "A Perspective on Keyless Inking," TAGA Proceedings, pp. 443-470.

Fadner, T. A. and Bain, L. J
1989 "Worldwide Status and Progress of Lithographic Keyless Inking Technologies," TAGA Proceedings, pp. 545-568.

Guerrette, D. J.
1985 "A Steady State Inking System Model for Predicting Ink Film Thickness Distribution," TAGA Proceedings, pp. 404-425.

MacPhee, J.
1998 "Fundamentals of Lithographic Printing" (GATF Press, Pittsburgh), Vol. I, Chapter 4.

MacPhee, J., Kolesar, P., and Federgun, A.
1986 "Relationship Between Ink Coverage and Mean Ink Residence Time in the Roller Train of a Printing Press," Adv. Printing Sci. Tech., Vol. 18, pp. 297-317.

Neuman C. P. and Almendinger, F. J.
1978 "Experimental Model Building of the Lithographic Printing Process III," GATF Annual Research Department Report, pp. 181-207.

Niemiro, T. and Chou, S. M.
1998 "A Simple Model for Appraising Keyless Offset Press Performance," submitted for presentation at the International Symposium on Printing and Coating Technology, University of Wales Swansea, UK.

Scheuter, K. R. and Rech, H.
1970 "About Measurement and Computation of Ink Transfer in Roller Inking Units of Printing Presses," TAGA Proceedings, pp. 70-87.

VanKanegan, E.
1998 "Goss Offset Inkers: Three Decades of Development," presented at the Metro Users Association Meeting in Orlando, Florida in February.